

# Microresonator-Based Optical Frequency Combs

T. J. Kippenberg,<sup>1,3\*</sup> R. Holzwarth,<sup>2,3</sup> S. A. Diddams<sup>4\*</sup>

The series of precisely spaced, sharp spectral lines that form an optical frequency comb is enabling unprecedented measurement capabilities and new applications in a wide range of topics that include precision spectroscopy, atomic clocks, ultracold gases, and molecular fingerprinting. A new optical frequency comb generation principle has emerged that uses parametric frequency conversion in high resonance quality factor ( $Q$ ) microresonators. This approach provides access to high repetition rates in the range of 10 to 1000 gigahertz through compact, chip-scale integration, permitting an increased number of comb applications, such as in astronomy, microwave photonics, or telecommunications. We review this emerging area and discuss opportunities that it presents for novel technologies as well as for fundamental science.

The optical frequency comb (1, 2) provides the “light gear” that enables a reliable and accurate means of counting optical cycles on the femtosecond ( $10^{-15}$  s) time scale, as required for the realization of optical clocks (3). The accuracy of such clocks is now measured to the 18th digit, exceeding the performance of their microwave counterparts by more than an order of magnitude (4). This development involves the measurement of the energy structure of atoms at an unprecedented level, allowing some of the most precise laboratory tests of the physics governing these systems (5, 6). Beyond their use in optical clocks and precision spectroscopy, frequency combs have found widespread use in various emerging research areas, including attosecond pulse generation, ultraviolet and infrared (IR) spectroscopy (7–9), precision distance measurement (10), remote sensing, optical waveform (11) and microwave signal synthesis (12), and astronomical spectrograph calibration (13, 14). These applications all benefit from the broad spectral coverage of the precisely controlled frequency components that constitute the optical comb.

To date, most of these applications have been realized with optical frequency combs based on femtosecond lasers—principally Ti:sapphire, Er:fiber, and Yb:fiber mode-locked lasers. Although fiber lasers have enabled optical frequency combs to evolve into a robust turnkey and commercial technology, for many interesting applications it would be advantageous to further reduce the footprint and at the same time to increase the repetition rate into the frequency range above 10 GHz. In recent years, a new comb generation principle has emerged that uses parametric frequency

conversion in compact optical microresonators (15). This approach may provide a new generation of combs that enable planar integration and may permit a direct link from the radio frequency (RF) to optical domain on a chip.

## Principles of Frequency Combs

It is instructive to briefly review the fundamental principles of optical frequency combs based on mode-locked lasers (1, 16). The frequency domain spectrum of the output of a mode-locked laser constitutes an optical frequency comb. The comb arises from the periodic train of pulses emitted

from such a laser (Fig. 1A). The spacing of the comb modes is given by the repetition rate ( $f_r$ ) of the laser, which is the inverse of the time required for an optical pulse to circulate through the laser cavity. Successive pulses emitted from a mode-locked laser are not generally identical. The difference between phase and group velocity in dispersive media inside the laser cavity causes the pulse envelope to slip with respect to the carrier phase from pulse to pulse (Fig. 1A inset), leading to a global offset of the frequency comb ( $f_o$ ). Correspondingly, the frequencies of the optical modes are then given by  $f_n = f_o + n \times f_r$ , where  $n$  is a large integer mode index (e.g.,  $n \sim 10^6$  for  $f_r = 100$  MHz and an optical frequency  $f_n \sim 10^{14}$  Hz). Measurement and frequency control of  $f_r$  and  $f_o$  (17–19) therefore provide a direct phase-coherent link between optical and RF domains, which is the basis of many frequency comb applications.

## Frequency Comb Generation Using Microresonators

Combs can also be produced from a continuous wave (CW) laser through the nonlinear optical process of parametric frequency conversion (Fig. 1, B and C) in optical microresonators (15) that trap and confine light in small volumes and thereby enhance the light intensity and nonlinear interaction (20). An important class of microresonators are whispering gallery mode (WGM) resonators—such as microdisks, microspheres, microtoroids, or microrings—which confine light by total internal reflection around the perimeter of an

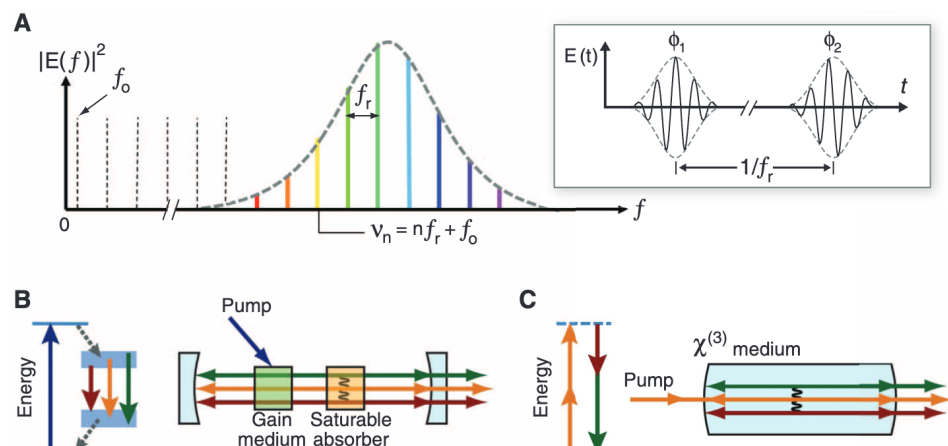


**Fig. 1.** (A) Time and frequency domain representation of an optical frequency comb. The mode spacing is given by the pulse repetition rate ( $f_r$ ), and the offset frequency ( $f_o$ ) describes the evolution of the carrier-envelope phase  $\Delta\phi = \phi_2 - \phi_1$ , which is the difference in phase between the pulse envelope and carrier between successive pulses (see inset). This phase difference ( $\Delta\phi$ ) leads to a global offset of the frequency comb given by  $f_o = f_r \Delta\phi/(2\pi)$ . (B) Conventional frequency comb generators based on mode-locked lasers, which—due to their pulsed operation—emit a comb of optical frequencies. Mode-locked lasers typically contain a gain medium (externally pumped, green arrow), a medium that induces mode locking (such as a saturable absorber), and a laser cavity. (C) Schematic of the parametric optical frequency comb generation method (15). The pump laser is part of the optical comb and injected into a resonator. Although a linear resonator cavity is shown here, in many situations, the resonator comprises a whispering-gallery mode microresonator. In contrast to the laser oscillator that has its gain medium pumped into an excited state and emits photons via stimulated emission, in the parametric oscillator the  $\chi^{(3)}$  nonlinear material has no energy storage but acts to convert two pump photons into signal and idler photons through virtual energy levels. This process is mediated by the intensity dependent refraction index  $n_2$  (also termed Kerr coefficient).

<sup>1</sup>Swiss Federal Institute of Technology Lausanne (EPFL), Lausanne, CH-1015, Switzerland. <sup>2</sup>Menlo Systems GmbH, Martinsried, Germany. <sup>3</sup>Max Planck Institut für Quantenoptik, Garching, Germany. <sup>4</sup>National Institute of Standards and Technology (NIST), Boulder, CO 80305, USA.

\*To whom correspondence should be addressed. E-mail: tobias.kippenberg@epfl.ch (T.J.K.); scott.diddams@nist.gov (S.A.D.)

air-dielectric interface. It has been first demonstrated in optical microspheres (21) that ultrahigh  $Q$  resonances ( $>100$  million) can be attained (where  $Q = \omega\tau$ , the resonance quality factor, with  $\tau$  denoting the photon storage time and  $\omega$  the optical angular frequency). This ultrahigh  $Q$  factor results in long interaction lengths and can lead to extremely low thresholds for nonlinear optical effects (sub micro-Watt power level). The optical WGM resonances correspond to an integer number of optical wavelengths (the mode index  $n$ ) around the microresonator's perimeter and are separated by the free spectral range (FSR), that is, the inverse round trip time in the cavity (Fig. 2C).

In the case of resonators made of fused silica, silicon, or crystals that exhibit inversion symmetry, the elemental nonlinear interaction is third-order in the electric field, which gives rise to the process of parametric four-wave mixing (FWM). This frequency conversion process originates from the intensity-dependent refractive index,  $n_0 + I \times n_2$ , where  $n_2$  is the Kerr coefficient,  $n_0$  is the linear refractive index, and  $I$  denotes the laser intensity. When a microresonator made from a third-order nonlinearity material is pumped with a CW laser (Figs. 1C and 2A), this parametric frequency conversion will annihilate two pump photons (with angular frequency  $\omega_p$ ) and create a new pair of photons: a frequency upshifted signal ( $\omega_s$ ), and a frequency downshifted idler ( $\omega_i$ ). The conservation of energy ( $2\hbar\omega_p = \hbar\omega_i + \hbar\omega_s$ , where  $\hbar$  is the reduced Planck constant) implies that the frequency components are equally spaced with respect to the pump (i.e.,  $\omega_s = \omega_p + \Omega$  and  $\omega_i = \omega_p - \Omega$ , where  $2\Omega$  is the frequency separation of the two new sidebands). If the signal and idler frequencies coincide with optical microresonator modes (Fig. 2C), the parametric process is enhanced, resulting in efficient sideband generation. Momentum conservation is satisfied in this process, since the WGMs have a propagation constant  $\beta = n/R$  (where  $n$  is the mode index and  $R$  the resonator radius) such that  $2\beta_p = \beta_s + \beta_i$  for symmetrically spaced modes [i.e., signal and idler modes differing by an equal amount (Fig. 2C)].

The generated sidebands have a defined phase relationship, that is, the relative phases of signal and idler with respect to the pump are fixed. If the scattering rate into the signal and idler modes exceeds their respective optical cavity decay rates ( $\kappa$ ) (Fig. 2C), parametric oscillation occurs, leading to symmetric sidebands that grow in intensity with increasing pump power. Although these effects are well known in nonlinear optics, such a process was demonstrated only recently in silica (22) and crystalline (23) microresonators. The advantage of microresonators is that the threshold for initiation of parametric oscillation can be strongly reduced, because the threshold scales with the inverse  $Q$  factor squared, implying that high  $Q$  can give a dramatic reduction in required optical power.

Parametric oscillations can also lead to spectra that contain multiple sidebands. The spectral band-

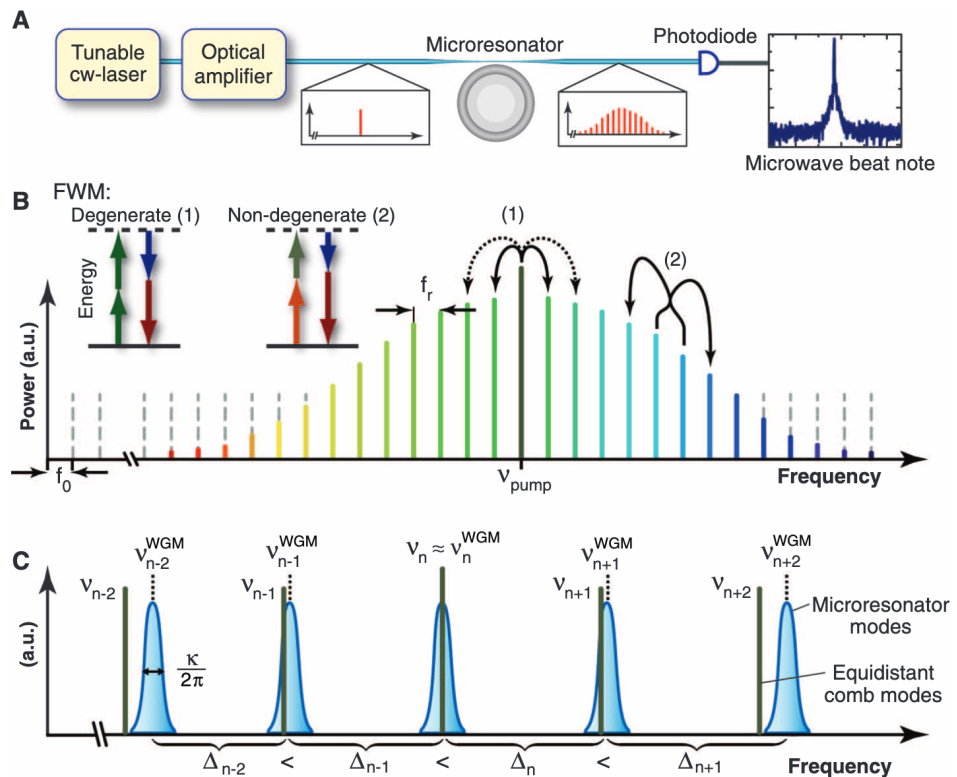


**Fig. 2.** Principle of optical frequency comb generation using optical microresonators. **(A)** An optical microresonator (here, a silica toroid microresonator) is pumped with a CW laser beam. The high intensity in the resonators ( $\sim \text{GW/cm}^2$ ) gives rise to a parametric frequency conversion through both degenerate and nondegenerate (i.e., cascaded) FWM. Upon generation of an optical frequency comb, the resulting beatnote (given by the inverse cavity round-trip time) can be recorded on a photodiode and used for further stabilization or directly in applications. **(B)** Optical frequency comb spectrum, which is characterized by the repetition rate ( $f_r$ ) and the carrier envelope frequency ( $f_0$ ). In the case of a microresonator-based frequency comb, the pump laser is part of the optical comb. The comb is generated by a combination of degenerate FWM (process 1, which converts two photons of the same frequency into a frequency upshifted and downshifted pair of photons) and nondegenerate FWM (process 2, in which all four photons have different frequencies). The dotted lines indicate degenerate FWM into resonator modes that differ by more than one mode number. The presence of cascaded FWM is the underlying process that couples the phases of all modes in the comb and allows transfer of the equidistant mode spacing across the entire comb. **(C)** Schematic of the microresonator modes (blue) and the frequency comb components (green) generated by pumping a whispering-gallery mode with a pump laser. The mode index ( $n$ ) refers to the number of wavelengths around the microresonator's perimeter. The FWM process results in equidistant sidebands. The bandwidth of the comb is limited by the variation of the resonator's free spectral range ( $\Delta_n$ ) with wavelength due to dispersion (shown is the case of anomalous dispersion).

width can be increased by two nonlinear processes (Fig. 2B). First, the pump laser can convert pump photons to secondary sidebands, spaced by multiple free-spectral ranges of the cavity (Fig. 2B). This degenerate FWM process would again lead to pairwise equidistant sidebands. However, the generated pairs of sidebands are not necessarily mutually equidistant, that is, they are not required to have the same frequency separation, as is needed to form a comb.

On the contrary, in a second process, comb generation can occur when the generated signal and idler sidebands themselves serve as seeds for further parametric frequency conversion, which is also referred to as cascaded FWM (also termed nondegenerate FWM because the two pump photons have different frequencies) (Fig. 2B). When signal and idler sidebands have comparable pow-

er levels to that of the pump inside the cavity, cascaded FWM is the dominant process by which new sidebands are generated. This process leads to the generation of equidistant sidebands, that is, all generated frequency components have the same separation from each other, giving rise to an optical frequency comb.

Dispersion, the variation of the free spectral range of the cavity with wavelength, ultimately limits this conversion process and leads to a finite bandwidth of the comb generation process because the cascaded FWM is less efficient once the comb modes are not commensurate with the cavity mode spectrum (Fig. 2C). Interestingly, however, the bandwidth of the comb is not entirely determined by the dispersion of the microresonator alone. Indeed, the nonlinear optical mode pulling (22) that occurs due to the Kerr nonlinearity at

high power plays an important role and thereby extends the comb beyond the limits imposed by dispersion alone (24).

An important aspect of the optical frequency comb in metrology is the stabilization of the comb repetition rate and carrier envelope frequency. Although microresonators do not feature any moveable parts, high-speed control of both  $f_o$  and  $f_r$  can be attained in an independent manner (25). In particular,  $f_o$  is directly accessible by varying the pump laser frequency with respect to the cavity mode. In contrast, the repetition rate can be varied by use of the intensity-dependent round-trip time of the cavity. Due to both thermal effects (i.e., the change of refractive index due to heating by absorbed laser power) and the Kerr nonlinearity, power variations of the laser are converted to variations in the effective path length of the microresonator and therefore change the mode spacing of the frequency comb (25). By using electronic feedback on both laser frequency and laser power, a microresonator Kerr comb with a mode spacing of 88 GHz has been fully frequency stabilized, with an Er:fiber laser-based frequency comb serving as reference.

### Experimental Systems: From Microtoroids to Integrated Chip-Scale Combs

The requirements for optical comb generation with a microresonator are a high  $Q$  cavity with small mode volume that is made from a material with a third-order nonlinearity and low dispersion. Examples of different resonators are shown in Fig. 3D. Toroidal microresonators (26) were the first system in which optical frequency comb generation was demonstrated (15). They consist of a microscale silica toroidal WGM and can attain  $Q$  factors in excess of 100 million (where  $Q$  is the product of optical angular frequency and photon lifetime). Highly efficient coupling into these planar devices can be achieved by using the evanescent field of tapered optical fibers (i.e., fibers whose diameter is less than, or on the order of, an optical wavelength in diameter, as illustrated in Fig. 2A). Overcoupling, the regime where the total cavity losses are dominated by useful output coupling “loss” into the fiber waveguide, has been achieved, which is important to attain high conversion efficiency, as only outcoupled comb components are detected. Using tapered fiber coupling of ~100 mW pump power at 1550 nm, a 375-GHz repetition rate frequency comb was attained with a spectral bandwidth exceeding 350 nm (15). This broad bandwidth was achieved with intrinsic dispersion compensation. A typical WGM microresonator features normal dispersion (i.e., high optical frequencies propagate slower than low optical frequencies), because a high-frequency mode will have its field maximum closer to the cavity boundary than a low frequency mode. This can be compensated with the material dispersion of silica that exhibits opposite behavior leading to a zero dispersion wavelength in the 1550-nm region. Pumping around this wavelength leads to the creation of broad

frequency combs that can exhibit more than a full octave (a factor of two in frequency), i.e., a span from 1000 to 2200 nm in wavelength as shown in Fig. 3A (24). That the emission indeed constitutes an optical frequency comb has been verified experimentally using multiheterodyne spectroscopy (9). The uniformity of the mode spacing was shown to be better than 1 part in  $10^{17}$  (15). These developments in microresonator-based combs have therefore closely followed the early work in femtosecond laser-based frequency combs, which was equally focused to verify the comb modes’ equidistant mode spacing at a similar level of precision (1).

A different class of resonators amenable to optical frequency comb generation are crystalline resonators (23). These are millimeter-scale resonators, made by polishing a cylindrical blank, that feature exceptional  $Q$  factors that exceed  $10^{10}$  and lead to an optical finesse  $>10^7$ . Input and output coupling of light is achieved with evanescent prismatic couplers, and optical frequency combs with a mode spacing as low as 12 GHz have been attained (27). This frequency is low enough to be directly detected using a photodetector, and such microresonators have been employed to generate microwave signals having high spectral purity (25, 28).

In addition to whispering gallery microresonators, Fabry-Perot fiber-based cavities can equal-

ly give rise to optical comb generation (29) by using an interplay of the third-order nonlinearity and Brillouin scattering. The Brillouin effect is due to the scattering of a photon by an acoustic phonon in the glass fiber and normally leads to a reflected field with a lower frequency (shifted by the phonon frequency of ~10 GHz in the case of silica). Because the acoustic phonons in most conventional materials (such as glass) are rapidly damped, Brillouin scattering is normally a phase-insensitive process. However, in the case of strongly cascaded Brillouin scattering (and in the simultaneous presence of FWM), even this process can lead to the emission of a comb of phase-locked frequency components.

Optical frequency combs have also been generated in more compact silicon photonic circuits that integrate both resonator and waveguide on the same chip. An important advance in this direction has been the recent demonstration of optical frequency comb generation in integrated silicon nitride (SiN) resonators (30) fabricated using approaches compatible with widespread complementary metal-oxide semiconductor (CMOS) technology. Although the optical  $Q$  factor remains many orders of magnitude lower ( $Q = 10^5$  to  $10^6$ ) than in the case of silica or crystalline resonators, this is partially compensated for by the tight confinement of the field inside the microresonators

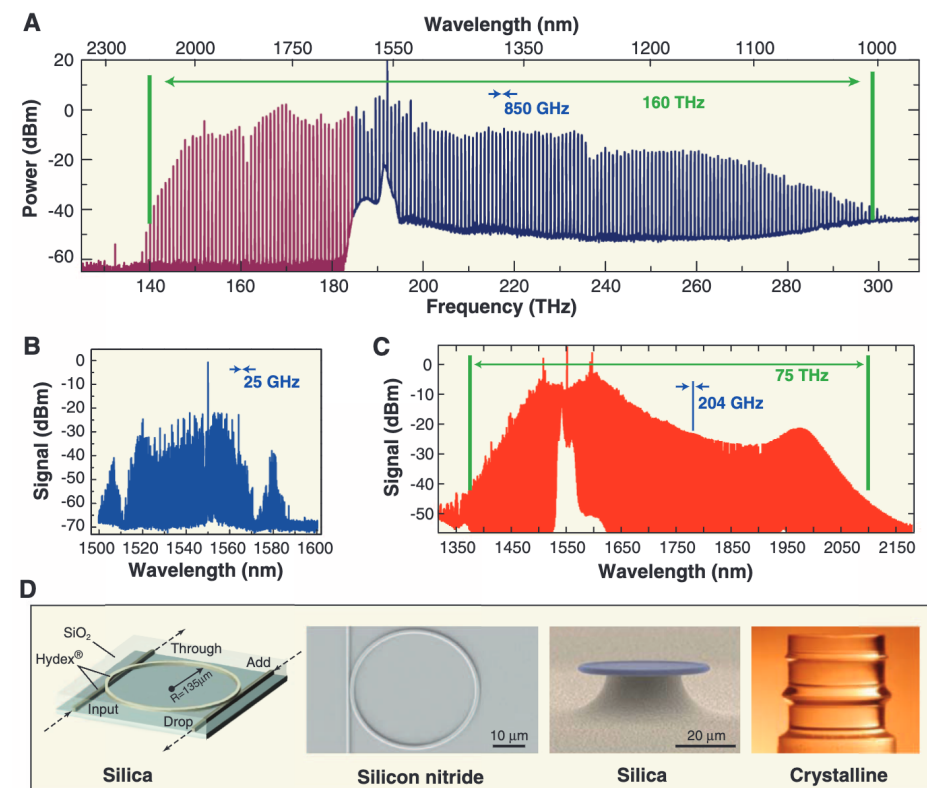


**Fig. 3.** Microresonator-based frequency combs. (A) Spectrum of an octave-spanning frequency comb generated using a silica microtoroidal resonator (24). (B) An optical frequency comb generated using a crystalline  $\text{CaF}_2$  resonator with a mode spacing of 25 GHz (27). (C) Optical spectrum covering two-thirds of an octave (with a mode spacing of 204 GHz) generated using an integrated SiN resonator (31). (D) Experimental systems in which frequency combs have been generated (from left to right): Silica waveguides on a chip (Hydex glass) (32), chip-based silicon nitride (SiN) ring resonators (30) and waveguides, ultrahigh  $Q$  toroidal microresonators (24) on a silicon chip, and ultrahigh  $Q$  millimeter-scale crystalline resonators (27).

(Fig. 3) and the fact that SiN exhibits a third-order nonlinearity of  $n_2 = 2.5 \times 10^{-15} \text{ cm}^2/\text{Watt}$ , which is approximately one order of magnitude larger than that of silica or crystalline materials such as CaF<sub>2</sub> or MgF<sub>2</sub>.

The main benefit of this approach is that it is fully planar and offers considerable flexibility, such as access to dispersion engineering through suitable resonator coatings. Moreover, this approach allows direct integration of the waveguide on the same chip-scale platform providing a means to fabricate a compact packaged device. Using an integrated SiN resonator, optical frequency comb generation has recently been demonstrated in this manner (31). As shown in Fig. 3, two-thirds of an octave with mode spacing of 204 GHz could be attained when pumping at 1550 nm with 300 mW of CW power (31). In addition, parametric comb generation has been demonstrated with another planar integrated resonator using a doped silica glass (Hydex) (32) that is also CMOS compatible and exhibited even higher optical *Q* factors ( $>10^6$ ).

Planar integration of a frequency comb is a considerable advance (30–32), but it is only part of a much broader class of systems that can be envisioned. In addition to high *Q* factor cavities and highly efficient coupling techniques, recent advances in silicon nanophotonics (33) have provided on-chip high-speed photodetectors, Raman lasers, modulators, and parametric gain (34). However, FWM near 1550 nm in silicon waveguides suffers from two-photon absorption, which induces optical loss. Thus, more efficient optical frequency comb generation in silicon could be expected in the range  $>2.2$  microns, which is below half the bandgap energy for silicon, suppressing two-photon absorption.

#### Emerging Applications for Microresonator Combs with High Repetition Rate

Frequency combs with high repetition rates (e.g., 10 to 1000 GHz) are desirable for a number of applications (Fig. 4), but generation is challenging with conventional mode-locked laser-based frequency combs due to the necessity of a short cavity length. In addition, the high repetition rate reduces the peak intensity of a pulse (the enhancement of the peak intensity scales approximately as the total number of comb lines). Nonetheless, repetition rates from ~10 GHz to greater than 100 GHz have been achieved in several laser systems (16), notably solid-state mode-locked lasers. The spectral bandwidths of these lasers are typically small ( $\Delta\lambda/\lambda < 1\%$ ), and as a result the peak powers have been insufficient for substantial

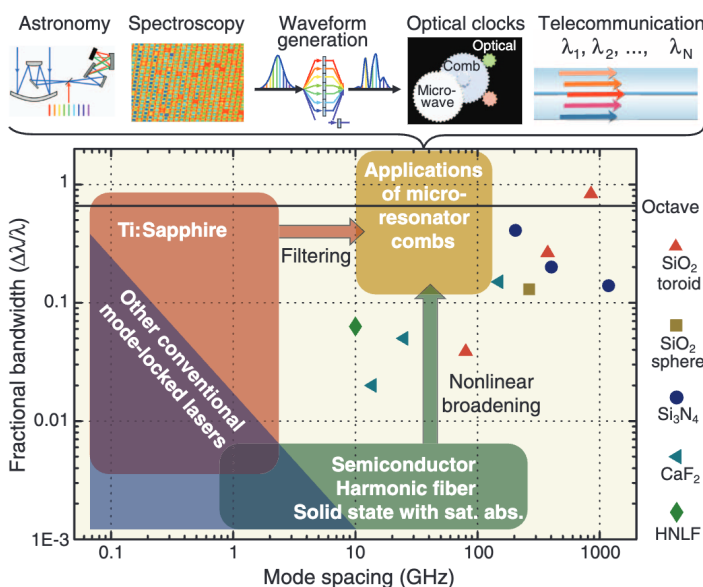


**Fig. 4.** Optical frequency comb technologies as a function of their mode spacing and fractional bandwidth (where  $\lambda$  denotes wavelength). The bandwidth in this case is defined approximately as the spectral width at which the power in the comb falls below a practically useful power of  $\sim 1 \text{ nW}$  per mode. The high-repetition-rate, large-bandwidth regime (gold colored) is presently approached by a variety of technologies and enables applications in astrophysical spectrometer calibration, telecommunications, optical arbitrary waveform generation, and spectroscopy. The stars denote a sampling of recently demonstrated microresonator-based frequency combs with corresponding material choice of the microresonator. This includes silica toroidal microresonators (15, 24, 25), silica microspheres (40), silicon nitride (31), crystalline CaF<sub>2</sub> resonators (27), and highly nonlinear fiber (HNLF) cavities (29). Applications of microresonator combs are illustrated at the top of the figure.

spectral broadening. One notable exception is a 10-GHz Ti:Sapphire laser that was spectrally broadened to cover an octave, thus enabling full frequency stabilization (35). Mode filtering of a comb with low repetition rate is another option to obtain higher repetition rates but comes at the expense of finite sidemode suppression (because filtering is not perfect), power reduction, and dispersion-induced spectral narrowing. In contrast, microresonator frequency combs naturally provide a high-repetition rate comb, which in some cases can span an octave (24). Although the crystalline resonators (27) have demonstrated mode spacings on the order of a few tens of Gigahertz, those achieved with SiN and silica microresonators are more typically in the range of a few hundred Gigahertz. Increasing the size of the microresonators lowers the repetition rate. However, this also implies that the *Q* factor of the cavity needs to increase as the radius of the resonator is increased in order to attain the same level of resonant power enhancement (i.e., optical finesse defined as free spectral range divided by the width of the resonance). A particularly interesting set of applications is present for combs with  $\Delta\lambda/\lambda > 10\%$  and a repetition rate in the 10 to 100 GHz range, where it is still possible to directly measure the repetition rate with a high-speed photodetector.

**Astronomical spectrograph calibration.** Precision spectroscopic measurements of periodic Doppler shifts in stellar spectra have led to the discovery of several hundred exoplanets over the past 15 years. Still, the detection of an Earth-like planet within the habitable zone of a distant star has been elusive. This is due in large part because the Doppler shift imparted by such a planet corresponds to a radial velocity of  $\sim 10 \text{ cm/s}$ , nearly an order of magnitude smaller than current detection limits. The ability to measure Doppler shifts near 1 cm/s may possibly allow direct observation of the acceleration of the expansion of the universe (13). Although astronomical spectroscopy with precision approaching  $10^{-10}$  requires numerous advances, it has been proposed that an optical frequency comb could provide a near-ideal calibration grid against which minute Doppler shifts could be measured. Key requirements for such a comb include broad spectral coverage, uniform power distribution, long-term stability, and a comb spacing of three to four times the resolution of the spectrograph. For a typical Echelle spectrograph in the visible or near-IR, the latter condition requires a mode spacing in the range of 10 to 30 GHz. Experiments using a low-repetition-rate laser that is filtered to transmit a sparse comb spectrum

have shown promising results (13, 14). However, a frequency-stabilized optical comb generated with a single laser and a microresonator could be potentially simpler, would be free of unsuppressed side-modes (compared to a filtered low-repetition-rate comb), and could be robustly packaged for unattended long-term operation. Combs with some of these qualities in the near-IR have already been generated in crystalline resonators (27).

**Telecommunications.** The use of optical frequency combs in the telecommunications bands covering 1450 to 1750 nm has been envisioned, but the channel spacing and data modulation rates pose strict requirements on the mode spacing and power levels. Due to the prevailing use of channels that are spaced by more than 10 GHz with power levels in the range  $>1 \text{ mW}$ , optical frequency combs have not penetrated into this domain. This could change as optical microresonator-based combs reliably generate combs that have high power per comb mode ( $>1 \text{ mW}$ ) and additionally can access repetition rates in the range of 25, 50, and 100 GHz, as required for high-capacity telecommunications. The advantage of the optical comb generator is that it can simultaneously generate hundreds of telecommunication channels from a single low-power off-chip source. Thus, a single high-power laser source and a microresonator-based comb can in principle replace the individual lasers used for each channel in telecommunications.

**Optical and microwave waveform synthesis.** A broad array of uniformly spaced comb modes with milli-Watt-level power would be valuable for applications in the field of microwave photonics and optical arbitrary waveform generation. The large mode spacing from a microresonator is advantageous for optical and microwave waveform generation (11), where recently developed approaches enable Fourier synthesis of user-designed optical waveforms via the control of amplitude and phase of each individual comb line (11). In the optical domain, this may enable generating complex or ultrashort (single cycle) waveforms, or potentially waveforms tailored for quantum control in atomic or molecular processes. When combined with high-speed photodetection, the agile manipulation of comb modes spaced by tens of Gigahertz also provides microwave and millimeter waveforms that are challenging, if not impossible, to synthesize with conventional techniques. Integration of the microresonator comb with advanced dispersive elements and modulators would provide maximal synthesizer functionality in a compact package. Finally, a free-running or stabilized microresonator comb has already been demonstrated to serve as a source of low-phase noise optical or microwave signals (12, 27).

**Frequency comb spectroscopy.** The fact that a frequency comb consists of a broad bandwidth array of what are essentially CW oscillators makes it an interesting source for directly probing atoms and molecules. Several spectroscopic approaches have been developed for conventional laser combs (36), and it is anticipated that a microresonator-based comb would bring new features of high mode power, compactness, and on-chip integration to this field. In one approach, the modes are spectrally resolved and their amplitudes reveal absorptive features characteristic of the sample gas (37, 38). An alternative multiheterodyne spectroscopy (9) requires two microresonator-based frequency combs (which may in principle reside on the same chip) having slightly differing repetition rates. One comb serves as a local oscillator, whereas the second comb traverses the sample and acquires the spectroscopic fingerprint. The resulting beatnotes of the two combs produce a radio frequency (RF) comb that contains a direct mapping of the optical spectrum, including any absorption and phase shift imparted by the sample (9, 39). Here, a trade-off exists; the high repetition rate gives fast acquisition times but entails coarse sampling of the absorption profile. Indeed, with mode spacing on the order of 10 GHz or greater, one could easily miss narrow spectral features. One solution to this problem would be to scan the microresonator comb, in which case the spectral resolution is ultimately given by the comb linewidth (38).

### Future Outlook: Challenges and Opportunities

Microresonator-based frequency combs are still in their development phase, and challenges must be overcome before their full impact is to equal that of femtosecond laser-based frequency combs.

At the same time, the parametric gain underlying these devices provides new opportunities.

One requirement for the use of microresonator combs in many frequency metrology applications will be a robust phase coherent link between RF and optical domains, as provided in the *f*-*2f* stabilization of femtosecond laser combs (17, 18). In practice, this requires a spectrum that spans an octave or an appreciable portion thereof. It is encouraging that octave-spanning spectra have already been generated in microtoroid resonators (24); however, an important outstanding aspect will be the frequency noise in the comb modes. Due to the small volume, many processes (such as thermo-refractive and thermo-elastic noise) are enhanced. Phase stabilization will only be viable when the noise on measured  $f_0$  and  $f_r$  beatnotes is sufficiently low to be compensated with servo-control techniques. A related issue for the planar waveguide and microtoroid systems discussed above is the reduction of  $f_r$  to a readily measured frequency below 100 GHz. The requirements of manageable noise processes, spectral coverage over a considerable portion of an octave, and  $f_r < 100$  GHz may represent the most important challenges to be overcome in the widespread use of microresonator frequency combs.

A key advantage of the parametric frequency conversion is that, in contrast to molecular and optical transitions of solid-state media, they exhibit broadband gain. Practically, the gain is only limited by the transparency window of the resonator material and dispersion, of which the latter can be engineered. In this context, it is interesting to consider optical comb generation from different materials. Semiconductors such as InP, Ge, SiN, or Si are transparent in the mid-IR. Hence, microresonator-based mid-IR combs could enable a new generation of optical sensing devices in the important spectroscopic “molecular fingerprinting” regime, with a multichannel generator and spectral analysis tools residing on the same chip. A challenge in this endeavor is the engineering of the optical resonators, such that their dispersion is sufficiently low while simultaneously maintaining a high *Q* factor. In this respect, crystalline resonators based on CaF<sub>2</sub> (23) appear highly promising. The transparency window of CaF<sub>2</sub> (or MgF<sub>2</sub>) ranges from 160 nm to ~8 μm, making this material highly interesting from the perspective of comb generation in the mid-IR (2500 nm onward) as well as wavelengths below 1000 nm.

### Summary

Research and development is under way that may allow not only a dramatic reduction in size but also access to comb generators with a repetition rate from 10s of GHz up to ~1 THz. For the technology to unfold, it will be necessary to combine the advances from nano- and microphtotonics (33) with those of frequency metrology. Microresonator comb generators are not likely to replace existing commercialized laser-based frequency comb generators but may well be the system of choice that can serve the demand for high repetition rates and wavelength ranges such as the

mid-IR. It is clear that the advances made in this rapidly developing field of optical microresonators may well advance optical frequency combs into new and still unanticipated application areas.

### References and Notes

- T. Udem, R. Holzwarth, T. W. Hänsch, *Nature* **416**, 233 (2002).
- S. T. Cundiff, J. Ye, *Rev. Mod. Phys.* **75**, 325 (2003).
- S. A. Diddams et al., *Science* **293**, 825 (2001).
- C. W. Chou, D. B. Hume, J. C. J. Koelemeij, D. J. Wineland, T. Rosenband, *Phys. Rev. Lett.* **104**, 070802 (2010).
- S. Blatt et al., *Phys. Rev. Lett.* **100**, 140801 (2008).
- T. Rosenband et al., *Science* **319**, 1808 (2008).
- C. Gohle et al., *Nature* **436**, 234 (2005).
- R. J. Jones, K. D. Moll, M. J. Thorpe, J. Ye, *Phys. Rev. Lett.* **94**, 193201 (2005).
- F. Keilmann, C. Gohle, R. Holzwarth, *Opt. Lett.* **29**, 1542 (2004).
- I. Coddington, W. C. Swann, L. Nenadovic, N. R. Newbury, *Nat. Photonics* **3**, 351 (2009).
- C. B. Huang, Z. Jiang, D. Leaird, J. Caraquita, A. Weiner, *Laser Photonics Rev.* **2**, 227 (2008).
- J. J. McFerran et al., *Electron. Lett.* **41**, 650 (2005).
- T. Steinmetz et al., *Science* **321**, 1335 (2008).
- G. H. Li et al., *Nature* **452**, 610 (2008).
- P. Del Haye et al., *Nature* **450**, 1214 (2007).
- U. Keller, *Nature* **424**, 831 (2003).
- H. R. Telle et al., *Appl. Phys. B* **69**, 327 (1999).
- D. J. Jones et al., *Science* **288**, 635 (2000).
- J. Reichert, R. Holzwarth, T. Udem, T. W. Hänsch, *Opt. Commun.* **172**, 59 (1999).
- K. J. Vahala, *Nature* **424**, 839 (2003).
- V. B. Braginsky, M. L. Gorodetsky, V. S. Ilchenko, *Phys. Lett. A* **137**, 393 (1989).
- T. J. Kippenberg, S. M. Spillane, K. J. Vahala, *Phys. Rev. Lett.* **93**, 083904 (2004).
- V. S. Ilchenko, A. A. Savchenkov, A. B. Matsko, L. Maleki, *Phys. Rev. Lett.* **92**, 043903 (2004).
- P. Del Haye et al., <http://arxiv.org/abs/0912.4890> (2009).
- P. Del Haye, O. Arcizet, A. Schliesser, R. Holzwarth, T. J. Kippenberg, *Phys. Rev. Lett.* **101**, 053903 (2008).
- D. K. Armani, T. J. Kippenberg, S. M. Spillane, K. J. Vahala, *Nature* **421**, 925 (2003).
- A. A. Savchenkov et al., *Phys. Rev. Lett.* **101**, 093902 (2008).
- A. A. Savchenkov et al., *Phys. Rev. Lett.* **93**, 243905 (2004).
- D. Braje, L. Hollberg, S. Diddams, *Phys. Rev. Lett.* **102**, 193902 (2009).
- J. S. Levy et al., *Nat. Photonics* **4**, 37 (2010).
- M. A. Foster et al., <http://arxiv.org/abs/1102.0326> (2010).
- L. Razzari et al., *Nat. Photonics* **4**, 41 (2010).
- J. Leuthold, C. Koos, W. Freude, *Nat. Photonics* **4**, 535 (2010).
- M. A. Foster et al., *Nature* **441**, 960 (2006).
- A. Bartels, D. Heinecke, S. A. Diddams, *Science* **326**, 681 (2009).
- M. C. Stowe et al., in *Advances In Atomic, Molecular, and Optical Physics*, E. Arimondo, P. R. Berman, C. C. Lin, Eds. (Academic Press, Burlington, MA, 2008), vol. 55, pp. 1–60.
- M. J. Thorpe, K. D. Moll, R. J. Jones, B. Safdi, J. Ye, *Science* **311**, 1595 (2006).
- S. A. Diddams, L. Hollberg, V. Mbele, *Nature* **445**, 627 (2007).
- I. Coddington, W. C. Swann, N. R. Newbury, *Phys. Rev. Lett.* **100**, 013902 (2008).
- I. H. Agha, Y. Okawachi, M. A. Foster, J. E. Sharping, A. L. Gaeta, *Phys. Rev. A* **76**, 043837 (2007).

**Acknowledgments:** The authors thank P. Del Haye and D. Heinecke for comments and preparation of the figures and A. Gaeta, L. Maleki, A. Matsko, and D. Moss for providing data and images. We further appreciate the thoughtful comments of S. Papp and D. Leibfried, T.J.K. and R.H. acknowledge support by a Marie Curie Industry-Academia Partnerships and Pathways, and T.J.K. acknowledges further support by the Swiss National Science Foundation, the National Centre of Competence in Research (NCCR) of Quantum Photonics, and the NCCR NanoTera. T.J.K. thanks T.W. Hänsch for support. S.A.D. acknowledges support from NIST.

10.1126/science.1193968